

# Laser-Machined Split-Ring Resonators Embedded in a Polymer Matrix for Glaucoma Monitoring <sup>†</sup>

Aybuke Calikoglu <sup>1</sup>, Gunhan Dundar <sup>1,2</sup>, Arda Deniz Yalcinkaya <sup>1,2</sup> and Hamdi Torun <sup>1,2,\*</sup>

<sup>1</sup> Department of Electrical and Electronics Engineering, Bogazici University, Bebek 34342, Istanbul, Turkey; aybuke.calikoglu@boun.edu.tr (A.C.); dundar@boun.edu.tr (G.D.); arda.yalcinkaya@boun.edu.tr (A.D.Y.)

<sup>2</sup> Center for Life Sciences and Technologies, Bogazici University, Kandilli 34684, Istanbul, Turkey

\* Correspondence: hamdi.torun@boun.edu.tr; Tel.: +90-212-359-6895

<sup>†</sup> Presented at the Eurosensors 2017 Conference, Paris, France, 3–6 September 2017.

Published: 17 August 2017

**Abstract:** This paper presents a biosensor based on laser-machined metallic split-ring resonators embedded in hydrophilic polymer matrices for glaucoma monitoring. The inner and outer radii of the annular resonators are optimized using a finite-element model for the anterior part of the fibrous layer of human eye. The split-ring resonators are designed to have resonant frequencies in S-band. The devices are fabricated by laser cutting of 15  $\mu\text{m}$ -thick aluminum sheets. Split-ring resonators are then embedded into photo-polymerized cross-linked hydrogels, which are used to prepare hydrophilic polymer matrices. The change in the resonance characteristics of the device is obtained with respect to the change in the curvature. The sensitivity of the sensor is calculated as  $-24.12$  MHz/mm per unit change in the radius of the curvature.

**Keywords:** split ring resonators; glaucoma monitoring; hydrogels; hydrophilic polymer matrices

## 1. Introduction

Glaucoma is one of the leading causes of blindness as it affects the optic disc and damages the optical nerve due to elevated intraocular pressure (IOP) [1] which is well correlated with the corneal radius of curvature [2]. A promising approach to monitor the progress of the disease is to monitor the IOP continuously and several invasive and noninvasive devices [3,4] have been developed using this approach.

Split-ring resonators (SRRs) are basic building blocks of metamaterials that may exhibit negative values of electric permittivity and magnetic permeability within a selected frequency range [5]. Proper electromagnetic excitations of SRRs result in electric and magnetic resonances, the frequency of which change due to the changes in the geometry of the structure. Thus, it is possible to utilize SRRs for continuous strain sensing as non-invasive and electrically passive sensors.

Hydrogels are biocompatible materials that are used frequently in the formulation of polymer matrices [6]. Hydrogel matrices have high water content and transparency which makes them suitable for soft contact lens fabrication. Moreover, preparing hydrogel-based polymer matrices in a laboratory environment is cost- and time-effective for custom applications.

In this application, SSRs embedded into 2-hydroxyethyl methacrylate (HEMA)-based hydrogel matrices are presented as non-invasive, low-cost and passive sensors for glaucoma monitoring. By photo-polymerization of polymer matrices and laser cutting of aluminum sheets, SRR-based devices were obtained in a simple, fast and cost-effective way. The presented method allows fabrication of disposable contact lens-based sensors. In addition, the thickness of the device can be adjusted to improve patient comfort since the sensor does not include any circuit or chip. Moreover, the contact lens-based sensors are electrically passive. These features offer significant advantages over similar sensors that include electronic chips that are embedded into contact lenses.

## 2. Design and Fabrication of the Sensors

The correlation between the IOP, corneal curvature and the resonant frequency of SRR determines the sensing mechanism in this application. An axisymmetric finite-element model, for the fibrous layer of the eye was modelled using COMSOL Multiphysics to investigate the effect of the change in the IOP on the corneal radius of curvature. In the model, the fibrous layer was assumed as an almost incompressible material with a linear elasticity in existence of small deformations. Mean values of the biomechanical model parameters are given in Table 1. The change in the curvature of the eye model for different values of IOP is shown in Figure 1. The placement of SRRs in a contact lens was determined where the displacement of the eyeball is maximum.

**Table 1.** Mean values of the fibrous layer parameters.

	Radius of Curvature (mm)	Thickness (mm)	Young's Modulus (MPa)
Central Cornea	7.34 [7]	0.494 [8]	1.4 [9]
Paracentral Cornea	7.69 [7]	0.532 [8]	1.64 [9]
Peripheral Cornea	8.15 [7]	0.607 [8]	1.52 [9]
Limbus	$\infty$ [9]	0.8 [10]	3 [9]
Sclera	12 [11]	0.6 [10]	7 [12]

<sup>1</sup> Corneal height = 2.4 mm, corneal diameter = 12 mm [13] ( $r = 0-1$  mm) ( $r = 1-3$  mm) ( $r = 3-5$  mm).

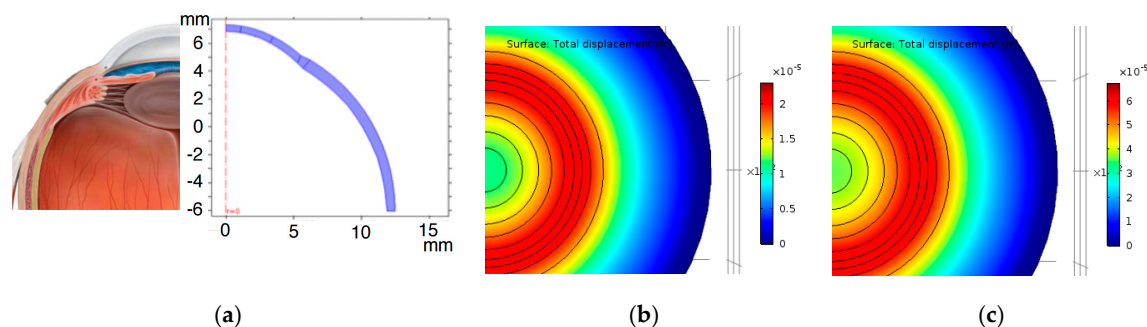


**Figure 1.** (a) 2D axisymmetric shape for 3D fibrous layer of the eye (unit of length is mm); (b) Simulated total displacements for  $\Delta$ IOP = 5 mmHg; (c) for  $\Delta$ IOP = 15 mmHg.

The dimensions of the SRRs were optimized for a resonant frequency of 3.5 GHz using CST Microwave Studio Software. The SRRs were shaped by laser cutting of 15  $\mu$ m-thick aluminum sheets. A sample SRR with inner radius of  $r = 4$  mm, width of  $w = 1.5$  mm and the gap distance of  $g = 150$   $\mu$ m is shown in Figure 2a. The SRRs were excited using a pair of monopole antennas, and the corresponding scattering parameters were measured using a vector network analyzer (VNA) (ZVB4, Rohde& Schwarz, Munich, Germany). The simulated and measured  $s_{21}$  parameters for a sample SRR are shown in Figure 2c. The quality factors of all resonators were characterized as  $Q > 1200$ .

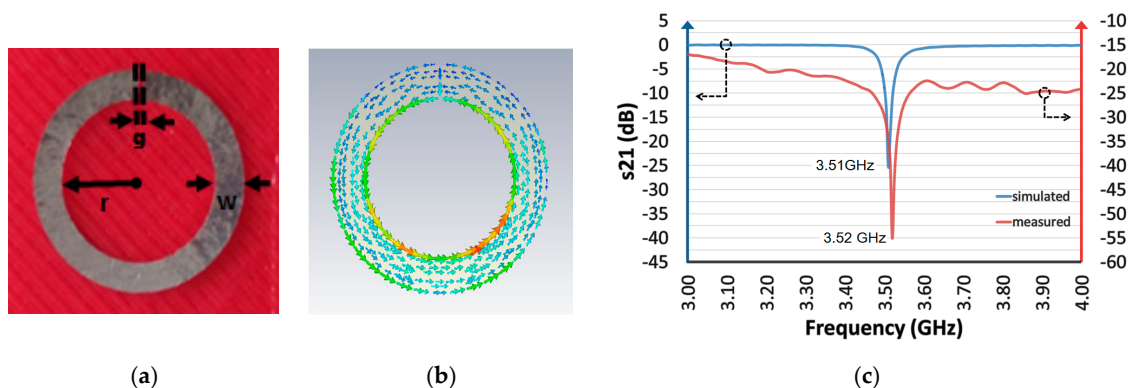


**Figure 2.** (a) A photograph of the sample SRR; (b) Simulated surface current density for this device at resonant frequency; (c) Simulated (blue) and measured (red)  $s_{21}$  spectra of the sample SRR.

The SRRs were then embedded into hydrogel matrices. HEMA and ethylene glycol dimethacrylate (EGDMA) were used as the monomer and cross-linker, respectively, for preparation of hydrogel matrices [15]. 65 wt % HEMA and 1 wt % EGDMA were first extracted from the inhibitors using basic alumina columns and were mixed with 1 wt % 2,2-dimethoxy-2-phenylacetophenone (DMPA) and 33 wt % H<sub>2</sub>O. The chemicals were obtained from Sigma-Aldrich (St. Louis, MO, USA). The mixture was stirred in a sonication bath for one hour. The SRR was carefully placed into the prepared solution between a pair of concave-convex glass molds, and the mixture was UV-cured for 12 min using 356 nm UV light (12 Watt). UV-cured sensor (Figure 3) was separated from the molds carefully and stored in DI water.

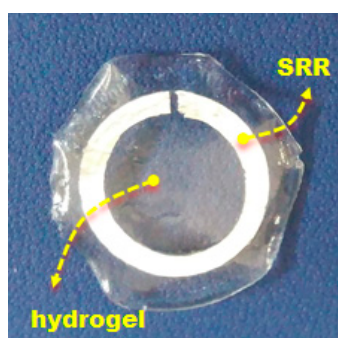


Figure 3. A photograph of an SRR embedded in the hydrogel matrix.

### 3. Experimental Setup and Results

An experimental setup has been constructed to measure the effect of curvature change of the final device on the scattering parameters simultaneously. An illustration of the experimental setup is shown in Figure 4a. First, a spherically deformed latex rubber was filled with de-ionized (DI) water and was connected to the tip of a syringe using a medical pipe. The syringe was used to pump additional DI water into this latex rubber balloon to change its radius of curvature. During the experiments, the outer surface of the spherical latex rubber was wet using distilled water and the SRR-based sensor was placed on top of it to mimic the effect of dielectric loading due to eye tear.

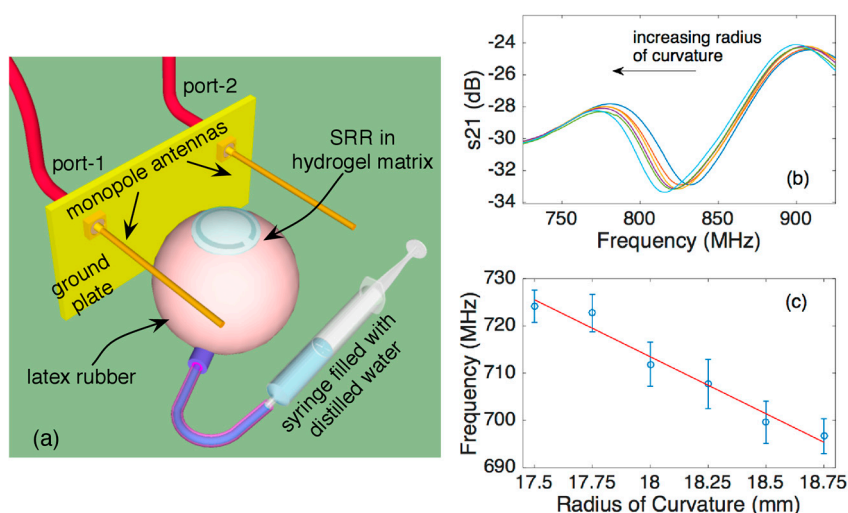


Figure 4. (a) An illustration of the experimental setup; (b)  $s_{21}$  spectra of the device as the radius of curvature increases; (c) Variation of the resonant frequency as a function of radius of curvature.

Figure 4b shows how the resonance behavior of the sensor alters with increasing radius of curvature. A sample SRR with inner radius of  $r = 5$  mm, width of  $w = 1.5$  mm and the gap distance of

$g = 3$  mm embedded in hydrogel matrix was used for this experiment. Latex rubber balloon was first filled with DI water to have spherical radius of 17.5 mm and the  $s_{21}$  spectrum of the device was measured. Then, the radius of curvature was increased by steps of 0.25 mm by pumping additional DI water into the balloon, while acquiring the  $s_{21}$  spectrum of the device. The resonant frequency of the sensor decreased monotonically during the experiment. The decrease in the quality factor of the device is due to the loss associated with water loading on the sensor. The experiment is repeated six times with the same device. The mean values and the standard deviation of the measured resonant frequencies given in Figure 4c. Based on the results, the sensitivity of the device was calculated as  $-24.12$  MHz/mm.

#### 4. Conclusions

In this work, we presented a biosensor application based on split-ring resonators embedded in a hydrogel based polymer matrix for glaucoma monitoring. Resonant frequency of the device exhibits monotonic change with respect to change in the radius of curvature and the sensitivity is obtained as  $-24.12$  MHz/mm. For the frequency resolution of 5 MHz, the change in the radius of curvature can be measured with the resolution of 207  $\mu\text{m}$ . The demonstrated SRR-based sensor is promising for non-invasive and continuous monitoring of glaucoma.

**Acknowledgments:** The Department of Scientific Research of Bogazici University under project 16A02TUG4.

**Conflicts of Interest:** The authors declare no conflict of interest.

#### References

1. Kingman, S. Glaucoma is second leading cause of blindness globally. *Bull. World Health Organ.* **2004**, *82*, 887–888, doi:10.1111/j.1755-3768.2008.01404.x.
2. Lam, A.K. The effect of an artificially elevated intraocular pressure on the central corneal curvature. *Ophthalmic Physiol. Opt.* **1997**, *17*, 18–24, PMID:9135808.
3. Samuels, B.; Cantor, L.B.; Ziaie, B. A Minimally Invasive Implantable Wireless Pressure Sensor for Continuous IOP Monitoring. *IEEE Trans. Bio-Med. Eng.* **2013**, *60*, 250–256, doi:10.1109/TBME.2012.2205248.
4. Leonardi, M.; Pitchon, E.M.; Bertsch, A.; Renaud, P.; Mermoud, A. Wireless contact lens sensor for intraocular pressure monitoring: Assessment on enucleated pig eyes. *Acta Ophthalmol.* **2009**, *87*, 433–437.
5. Veselago, V.G. The electrostatics of substances with simultaneously negative values of epsilon and mu. *Sov. Phys. Uspekhi* **1968**, *10*, 509–514, doi:10.1070/PU1968v010n04ABEH003699.
6. Ahmed, E.M. Hydrogel: Preparation, characterization, and applications: A review. *J. Adv. Res.* **2015**, *6*, 105–121, doi:10.1016/j.jare.2013.07.006.
7. Scott, A.R.; Michael, J.C.; Leo, G.C.; Ross, J.F. The Topography of the Central and Peripheral Cornea. *Investig. Ophthalmol. Vis. Sci.* **2006**, *47*, 1404–1415, doi:10.1167/iovs.05-1181.
8. Rapuano, C.J. Nine-point corneal thickness measurements and keratometry readings in normal corneas using ultrasound pachymetry. *Insight* **1993**, *18*, 16–22, PMID:8301187.
9. Hjortdal, J. Regional elastic performance of the human cornea. *J. Biomech.* **1996**, *29*, 931–942, doi:10.1016/0021-9290(95)00152-2.
10. Vurgese, S.; Panda-Jonas, S.; Jonas, J.B. Scleral Thickness in Human Eyes. *PLoS ONE* **2012**, *7*, e29692, doi:10.1371/journal.pone.0029692.
11. Carvalho, L.A.; Prado, M.; Chamon, W. Keratoconus prediction using a finite element model of the cornea with local biomechanical properties. *Arq. Bras. Ophthalmol.* **2009**, *72*, doi:10.1590/S0004-27492009000200002.
12. Zhang, Y.; Li, Z.; Liu, L.; Han, X.; Zhao, X.; Mu, G. Comparison of Riboflavin/Ultraviolet-A Cross-Linking in Porcine, Rabbit, and Human Sclera. *BioMed. Res. Int.* **2014**, *2014*, 194204, doi:10.1155/2014/194204.

13. Anterior Segment Sagittal Height and Soft Contact Lens Fitting: New Thoughts, New Understandings. Available online: [http://www.softspecialedition.com/world\\_wide\\_vision\\_xii](http://www.softspecialedition.com/world_wide_vision_xii) (accessed on 28 June 2017).
14. Childs, A.; Li, H.; Lewittes, D.M.; Dong, B.; Liu, W.; Shu, X.; Sun, C.; Zhang, H.F. Fabricating customized hydrogel contact lens. *Sci. Rep.* **2016**, *6*, 34905, doi:10.1038/srep34905.



© 2017 by the authors. Licensee MDPI, Basel, Switzerland. This article is an open access article distributed under the terms and conditions of the Creative Commons Attribution (CC BY) license (<http://creativecommons.org/licenses/by/4.0/>).